The Armed Forces Institute of Pathology
Department of Veterinary Pathology

Conference Coordinator
Matthew Wegner, DVM

WEDNESDAY SLIDE CONFERENCE 2010-2011

Conference 1   **11 August 2010**

Conference Moderator:
COL (Ret.) John Pletcher, MPH, DVM, Diplomate ACVP

<u>**CASE I:**</u> SPRI Case 1 (AFIP 2941205).

Signalment: 2-year-old, female, Sprague-Dawley rat (*Rattus norvegicus*).

History: The animal was part of the vehicle control group of a two-year gavage carcinogenicity study.   A scheduled terminal necropsy was performed on day 731 of the test.
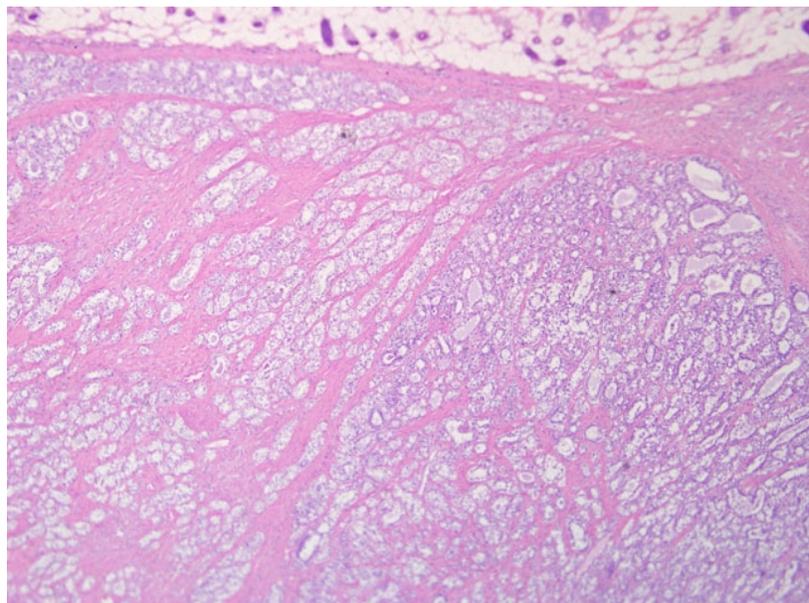
Gross Pathology: The terminal body weight was 339.1 grams.   The submitted tissues correlate with two masses located in the right inguinal region. These masses were dark red to tan, lobulated, and firm.   Other necropsy findings included an enlarged adrenal cortex, an enlarged pituitary compressing the ventral brain, and dark red foci throughout the liver.
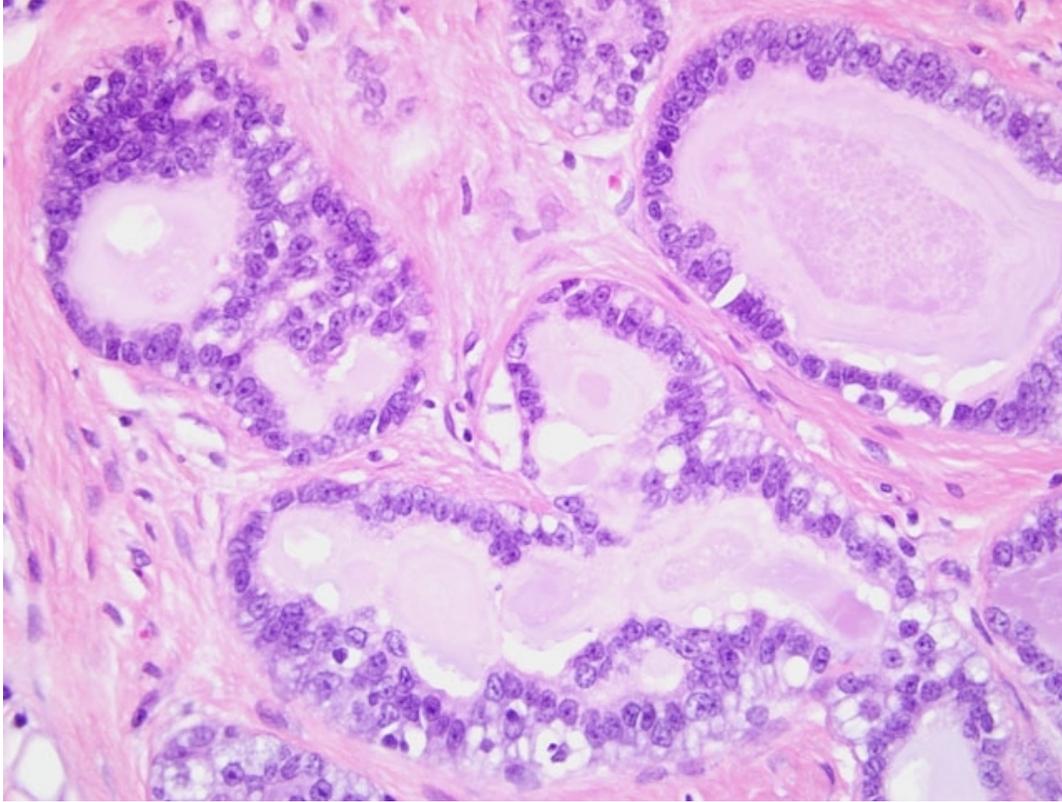
Laboratory Results: Not available.

Histopathologic Description: <u>Haired skin and mammary gland</u>: Histologically, there is an expansile, non-encapsulated but well-delineated mass within the subcutis, which compresses adjacent tissues. The mass is multilobulated with varying islands of epithelial cells separated by thick bands of dense fibrous connective tissue. Thin bands of connective tissue extend into some islands forming a trabecular pattern which separate the epithelial cells into small, single-cell lined acini and tubules while other islands have scant amounts of fibrous connective tissue and contain more dense

1-1. Haired skin, mammary gland, fibroadenoma, with atypia, rat.   There is an expansile, well-demarcated, multilobulated, neoplasm composed of epithelial cells arranged in islands, trabeculae, and tubuloacinar structures separated by dense bands of fibrous connective tissue. (HE 20X)

1-2. Haired skin, mammary gland, fibroadenoma, with atypia, rat. Neoplastic epithelial cells have moderate vacuolated cytoplasm and small dark nuclei; the lumina of tubuloacinar structures frequently contain secretory material. The surrounding fibrous connective tissue is composed of spindle cells with scant eosinophilic cytoplasm and small nuclei. (HE 400X)

accumulations and pilings of atypical epithelial cells which compress adjacent lobules. The epithelial cells within the trabeculae of connective tissue are well differentiated with small, dark nuclei and vacuolated cytoplasm, and lumena frequently contain basophilic secretory material. The fibrous connective tissue is also composed of well-differentiated cells with abundant streaming eosinophilic cytoplasm and small, dark nuclei. The atypical epithelial components which contain more densely cellular epithelial cells and less connective tissue also contain large ectatic pools of basophilic secretory material which are occasionally mineralized. These atypical epithelial cells exhibit mild to moderate anisocytosis with abundant basophilic to vacuolated cytoplasm and large, round, vesicular nuclei with one or two prominent magenta nucleoli. Mitotic figures are fewer than 1 per high magnification field. There is a minimal infiltrate of neutrophils scattered throughout the mass. Well developed blood vessels are common throughout the mass although clear evidence of metastatic invasion is not observed.

Contributor's Morphologic Diagnosis: Mammary glands: Adenocarcinoma arising in a fibroadenoma.

Contributor's Comment: Other significant findings in this animal included: adrenal gland cortical cell adenoma, contralateral cortical atrophy, cystic hemorrhagic degeneration; liver angiectasis and biliary ductular hyperplasia; pituitary gland pars distalis adenoma; ovaries atrophy; thymus atrophy; and uterus endometrial fibrosis. In this particular two-year study the incidence of mammary tumors in 100 control group females included 28 fibroadenomas, 3 adenomas, 25 adenocarcinomas, and 7 adenocarcinomas arising in fibroadenomas.

Mammary tumors are extremely common spontaneous lesions in aging rats although the incidence and type of tumor varies considerably from one rat strain to the next. Within the F344 strain, fibroadenomas are reported in up to 60% of females surviving the length of a two-year study.[2] The incidence of this same tumor in Wistar rats is 45% and in Sprague-Dawley rats ranges from 24-68% in females at the end of a two-year study.[4,5] In most of the common rat strains, adenocarcinomas are considerably less common than fibroadenomas. In toxicologic studies, this variation in tumor incidences between strains demonstrates the importance of relevant controls when assessing whether a tumor is test-article related or an incidental finding. Furthermore, this variation also suggests that there are important pathogenic distinctions between the strains to consider when using data from laboratory animals to evaluate human health risks. It has long been established that the quantity and ratio of estrogen to prolactin have a profound influence on the biological behavior of these tumors in rats.[5] In addition to xenobiotics, there are numerous environmental factors such as diet, pregnancy status, and housing conditions which can further influence these tumor incidences.

The criteria for classification of mammary tumors in the rat have been well described.[1] Additional clarification and refinement of diagnostic criteria have been accomplished to enhance uniformity of terminology among pathologists.[3] This harmonization is an important and ongoing process that is essential for accurate risk assessment by the various regulatory agencies throughout the world. In conjunction with this harmonization, continued monitoring of the incidence of spontaneous tumors in these various strains provides the opportunity for recognition of important biological shifts in tumor behavior over time.

AFIP Diagnosis: Haired skin, mammary gland: Mammary fibroadenoma, with atypia.

Conference Comment: Conference participants carefully considered the contributor's diagnosis of adenocarcinoma arising in fibroadenoma, which was included in the differential diagnosis, along with lobular hyperplasia, fibroadenoma, and fibroadenoma with atypia. Consistent with the contributor's description, the microscopic sections consist of haired skin and mammary gland containing an unencapsulated, well-demarcated, expansile mass composed of epithelial cells arranged in well-differentiated acini and tubules and separated by variable amounts of dense fibrous connective tissue stroma. Acini and tubules are generally lined by a single layer of neoplastic epithelial cells. Epithelial cells are cuboidal and have moderate amounts of vacuolated cytoplasm and round to oval, finely stippled nuclei and indistinct nucleoli. There are few mitotic figures. The fibrocollagenous stroma is composed of well-differentiated spindled cells with eosinophilic fibrillar cytoplasm and small, elongate nuclei. While some participants identified scattered mitoses and areas of epithelial atypia in the neoplasm, including piling up of epithelial cells in clusters of acini, based on the sections available for evaluation participants did not observe features indicative of adenocarcinoma, such as invasion through the basement membrane, desmoplasia, necrosis, high mitotic rate, clumped chromatin, bizarre mitoses, squamous metaplasia, or the histologic patterns associated with mammary adenocarcinoma in the rat (i.e. comedo, cribriform, or papillary).[3] That said, this lesion represents the difficulty in examination of numerous sections of a neoplasm, and the initial tissue sections evaluated by the contributor may well have contained areas demonstrating convincing adenocarcinoma within mammary fibroadenoma. The chart below summarizes key histologic features of the differentials as indicated in the Standardized System of Nomenclature and Diagnostic Criteria (SSNDC) Guide:[3]

Lobular hyperplasia	Lobular enlargement by histologically normal, hyperplastic alveoli Single layer of alveolar epithelium

Atypical hyperplasia	Focal irregular epithelial proliferation with cellular atypia and/or pleomorphism Formation of epithelial papillae, arches, nests or plaques projecting into the lumen
Adenoma	Well-circumscribed proliferation of clusters of tubuloacinar structures on a scanty collagenous stroma Alveoli lined by a single layer of epithelium with a small nucleus, one nucleolus and cytoplasm that is often vacuolated Papillary or cystic papillary patterns
Fibro-adenoma	Two morphologically distinct cell populations ± areas of atypia/cellular pleomorphism 1. Epithelium – single layer, uniform, with or without lipid vacuoles forming tubuloacinar structures or cysts 2. Fibrous connective tissue of variable density coursing within and between lobules with few fibrocytes
Adeno-carcinoma	Uniform epithelial cells varying from one to many cells thick; have a central round nucleus; clumped chromatin; one nucleolus and many mitoses May or may not be invasive Patterns include papillary, tubular, cribriform, or comedo
Adeno-carcinoma arising in a fibro-adenoma	Histologic pattern of adenocarcinoma Variable histologic pattern of fibroadenoma component

References:

1. Boorman GA, Wilson JT, van Zwieten MJ, Eustis SL: Mammary gland. *In*: Boorman GA, Eustis SL, Elwell MR, Montgomery CA, MacKenzie WF, eds. *Pathology of the*

Fischer Rat. San Diego, CA: San Diego Academic Press; 1990:298-305.

2. Haseman JK, Hailey JR, and Morris RW. Spontaneous neoplasm incidences in Fischer344 rats and B6C3F1 mice in two-year carcinogenicity studies: a national toxicology program update. *Toxicol Pathol.* 1998;26(3): 428-41.

3. Mann PC, Boorman GA, Lollini LO, McMartin DN, Goodman DG: Proliferative lesions of the mammary gland in rats. In: *Guides for Toxicologic Pathology*, accessed at http://www.toxpath.org/nomen/index.htm, 11 August 2010. Washington D.C.: Society of Toxicologic Pathologists/ American Registry of Pathology/The Armed Forces Institute of Pathology; 1996

4. Poteracki J, Wash KM. Spontaneous neoplasms in control Wistar rats: a comparison review. *Toxicol Sci.* 1998;45(1): 1-8.

5. Van Zwieten MJ, Hogenesch H, Majka JA, Boorman GA: Non-neoplastic and neoplastic lesions of the mammary glands. In: Mohr U, Dungworth DL, Capen CC eds. *Pathobiology of the Aging Rat* Volume 2. Washington D.C.: ILSI Press; 1994:459-475.

CASE II: PFIZER SDN CASE 2 (AFIP3135367).

Signalment: 6 to 8-week-old, male, Sprague-Dawley rat (*Rattus norvegicus*).

History: The rat was part of the high dose group of gentamicin nephrotoxicity study. Subcutaneous administration of gentamicin once daily at dose of 75 mg/kg/day for 7 days was performed. The rat was euthanized at day 8. No clinical abnormalities were detected. This study was conducted in accordance with the current guidelines for animal welfare (Animals [Scientific Procedures] Act, 1986 and ILAR Guide for the Care and Use of Laboratory Animals, 1996).

Gross Pathology: Both kidneys were pale and mildly enlarged with increased absolute weights (+22% relative to control) and relative weights (+23% relative to body weight).

Laboratory Results: A slightly increased creatinine concentration (17% above mean control values) at $\geq$ 75 mg/kg/day on day 8 was observed. There were no significant changes in blood urea nitrogen (BUN) concentrations.

Histopathologic Description: Kidney: Histologically, the section of kidney showed degeneration and necrosis of the epithelium of predominantly cortical tubules (most likely proximal convoluted tubules) characterized by presence of varying degrees of tubular epithelial vacuolar degeneration, attenuation, loss of epithelial cellular detail with abundant pyknotic nuclei and karyorrhectic debris (necrosis), and detachment from intact basement membranes. Multifocally, in association with these changes, were basophilic tubules characterized by epithelial cells with basophilic cytoplasm, vesiculate nuclei, and infrequent mitoses (regeneration) and

low to moderate numbers of mononuclear cells (lymphocytes and plasma cells) in the interstitium. There were occasional apoptotic epithelial cells and tubular casts (not observed in all submitted sections).

Contributor's Morphologic Diagnosis: Kidney: Moderate multifocal tubular epithelium degeneration and necrosis with mild regeneration.

Contributor's Comment: Gentamicin (GM) is a broad-spectrum aminoglycoside antibiotic used against life threatening bacterial infection. Its mechanism of action occurs by inhibition of bacterial protein synthesis mainly through binding with the 30S ribosomal subunit. It is well known as an inducer of acute nephrotoxicity which occurs in about 15-30% of treated animals.[1] The present case represents a classical GM-induced nephrotoxicity characterized predominantly by tubular degeneration/necrosis at the end of the dosing period on day 8.
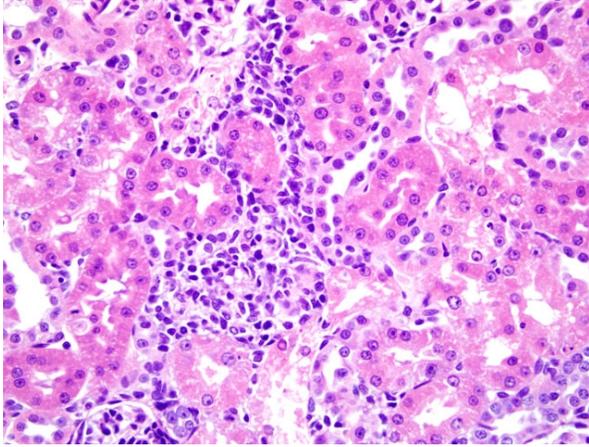
The key histopathological features of GM-treated animals are vacuolar degeneration and necrosis of renal proximal convoluted tubular epithelium in the cortex.[4,6] Ultrastructural changes of proximal tubule epithelial cells include damage and loss of brush borders, and formation of cytosegrosomes and myeloid bodies.[4,6] Gentamicin nephrotoxicity is reversible and regeneration of tubular epithelium may occur even during continued therapy.[4,6]

The underlying mechanism by which GM causes nephrotoxicity is not fully understood. However, one of the most important mechanisms for GM induced nephrotoxicity is reactive oxygen species-mediated.[2,5] It has been shown that GM generates reactive oxygen species which produce cellular injury and necrosis via peroxidation of membrane lipids, protein denaturation, and DNA damage in the kidney.[1,2] It has also been reported that GM suppresses antioxidant defense enzymes (e.g. superoxide dismutase, catalase and glutathione peroxidase) and increases lipid peroxidation in the renal cortex and medulla.[2,5]
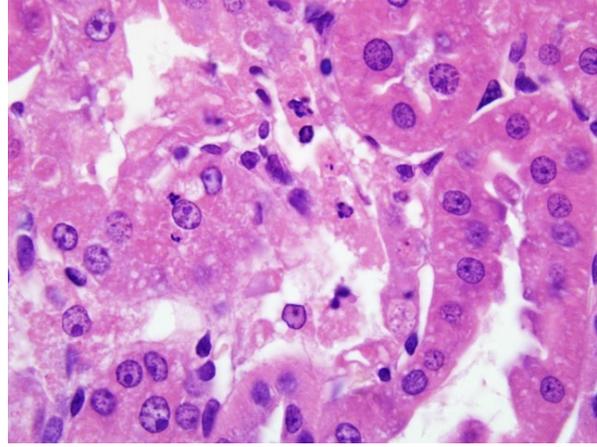
A recent interesting development is the attempt to use extracts from medicinal plants with antioxidant properties to ameliorate/protect against GM-induced nephrotoxicity in rats. Such medicinal plants include garlic, as well as diallyl sulfide, a compound isolated from garlic, *Nigella sativa* oil, Maidenhair tree extract (*Ginkgo biloba), Rhazya stricta* and green tea extract.[1,5,8]

AFIP Diagnosis: Kidney, cortex: Tubular degeneration and necrosis, multifocal, mild to moderate with regeneration and lymphoplasmacytic interstitial nephritis.

Conference Comment: Renal lesions attributable to toxins vary in severity based on dose, time, strain, sex, age, route of administration and degree of hydration. Animals with poor hydration often have higher drug concentrations in renal

2-1. Kidney, rat. Multifocally in the cortical interstitium, there are low to moderate numbers of lymphocytes, macrophages, and plasma cells that surround degenerate and necrotic tubules. (HE 400X)

2-2. Kidney, rat. Multifocally in the renal cortex there is tubular epithelial degeneration, attenuation, and necrosis. (HE 1000X)

tubular epithelium than well-hydrated animals, resulting in increased toxicity. Pale, enlarged kidneys, which bulge on cut surface and may have a white stripe in the outer stripe of the outer medulla, are indicative of acute tubular necrosis; chronically affected kidneys are often shrunken, irregular and pitted.

A focal point of discussion for conference participants was the histology of the rat kidney in relation to lesion distribution. Histologically, the rat kidney can be divided into five zones. Beginning with the capsular surface, these are: the cortex; the outer stripe of the outer medulla; the inner stripe of the outer medulla; the inner medulla; and the papilla. The proximal tubule is often subdivided into three segments: P1 and P2 contain the proximal convoluted tubule (PCT); and P3 represents the pars recta. While P1 and P2 are located in the cortex, the P3 segment is found in the outer stripe of the outer medulla. Accurate classification of renal lesions with respect to the structures affected and anatomic location can aid in determination of potential causes of renal tubular damage and associated mechanisms of action. The proximal tubule is often the site of toxic injury, with P3 most commonly affected. The histologic lesion patterns of acute renal tubular necrosis include: multifocal distribution, affecting individual cells or groups of tubules, such as with N-(4'-fluoro-4-biphenyl) acetamide; segmental distribution, such as when affecting only P3 (aminoglycosides, furans, thiophenes, acetaminophen, ochratoxin A and mercuric chloride); and multiple proximal tubule segments, such as that which occurs with uranyl nitrate and cisplatin.[7]

The moderator commented on the sexual dimorphism exhibited in rat kidneys. Cells within segments P1 and P2 in the male rat exhibit higher endocytic activity and have larger, more numerous lysosomes. Within the PCT of sexually mature males, cells frequently have eosinophilic cytoplasmic

granules composed of $alpha_{2U}$-globulins; visualization of these granules is enhanced by staining with the Mallory-Heidenhain stain.[3] Abnormal accumulation of these granules is referred to as "hyaline droplet nephropathy" and can be seen in male rats as a result of toxic changes, or in both sexes in association with disseminated histiocytic sarcoma.[3] Female rats have more extensive smooth endoplasmic reticulum in segments P1 and P2, which suggests higher mixed-function oxidase activity and enhanced metabolism of drugs.[7]

Contributor: Pfizer Limited, Drug Safety Research and Development (DSRD), Department of Toxicological Pathology, Sandwich, Kent CT13 9NJ, United Kingdom
http://www.pfizer.co.uk/Pages/Home.aspx

References:
1. Ali BH. Agents ameliorating or augmenting experimental gentamicin nephrotoxicity: some recent research. *Food Chem Toxicol*. 2003;41**:**1447-1452.
2. Banday AA, Farooq N, Priyamvada S, Yusufi, ANK, Khan F. Time dependent effects of gentamicin on the enzymes of carbohydrate metabolism, brush border membrane and oxidative stress in rat kidney tissues. *Life Sci*. 2008;82**:**450-459.
3. Hard GC, Alden CL, Bruner RH, Frith CH, Lewis RM, Owen RA, Krieg K, Durchfeld-Meyer B. Non-proliferative lesions of the kidney and lower urinary tract in rats. In: *Guides for Toxicologic Pathology*, accessed at http://www.toxpath.org/nomen/index.htm, 11 August 2010. Washington D.C.: Society of Toxicologic Pathologists/American Registry of Pathology/The Armed Forces Institute of Pathology; 1999.
4. Houghton DC, Harnett M, Campbell-Boswell M, Porter G, Bennett WM. A light and electron microscopic analysis of

gentamicin nephrotoxicity in rats. *Am J Pathol*. 1976;82:589–612.

5. Khan SA, Priyamvada S, Farooq N, Khan S, Khan MW, Yusufi ANK. Protective effect of green tea extract on gentamicin-induced nephrotoxicity and oxidative damage in rat kidney. *Pharmacol Res*. 2009;59:254-262.

6. Mingeot-Leclerq M, Tulkens PM. Aminoglycosides: nephrotoxicity. *Antimicrob Agents Chemother*. 1999;43(5): 1003–1012.

7. Montgomery CA Jr., Seely JC: Kidney. In: Boorman GA, Eustis SL, Elwell MR, Montgomery CA, MacKenzie WF, eds. *Pathology of the Fischer Rat*. San Diego, CA: San Diego Academic Press; 1990:127-153.

CASE III: 08/006 (AFIP 3136051).
Signalment: 82-week-old, female, Wistar Rat, rat (*Rattus norvegicus*).

History: This specific-pathogen-free rat was part of a carcinogenicity study as a sentinel. The rat was euthanised because of wasting, rectal prolapse and a palpable caudal abdominal mass.

Gross Pathology: At necropsy, a well-demarcated, round mass of five centimetres in diameter was present in the distal part of the uterus and the anterior part of the vagina and adherent to the rectum. It was polycystic, soft, dark to brown with multiple foci of necrosis. No other significant gross lesion was noted.

Histopathologic Description: Vagina: The mass is an ill-demarcated, non-encapsulated, infiltrating cellular proliferation involving diffusely the serosa, the tunica muscularis, the lamina propria and the epithelium which was ulcerated. The mass is moderately cellular, made of sheets of loosely packed ovoid to spindled cells separated by large amounts of pale, eosinophilic, finely fibrillar matrix with numerous blood vessels. There are numerous, disseminated, variable-sized (0.1 mm to 1 cm) cavities containing eosinophilic, reticulate, amorphous material admixed with foamy macrophages or erythrocytes and lined by closely packed neoplastic cells resembling epithelium (pseudocysts). The cells have indistinct cell borders, moderate amount of pale, eosinophilic cytoplasm, oval to fusiform, centrally-located nucleus with reticulate to hyperchromatic chromatin and one small nucleolus; the neoplastic cells surrounding the pseudocysts appear polarized with a basal nucleus. The cells have mild poikilocaryosis and anisokaryosis. Mitotic figures are rare: mean 1 per HPF (40X) with a maximum of 2. There are multifocal areas of coagulation necrosis. Few lymphocytes, plasma cells and siderophages are scattered within the mass. The lumen is filled with cellular debris, purulent exudate and bacterial colonies.

Uterine horn: The same neoplasm extends from the serosa to the lamina propria. The lumen is filled with pus.

3-1. Vagina; uterus; and rectum, Malignant schwannoma, rat. There is a well demarcated, round mass in the distal part of the uterus and the anterior part of the vagina adherent to the rectum. Photograph courtesy of Ecole Nationale Veterinaire D'Alfort, Unite d'histologie et d'Anatomie Pathologique, 7, Avenue du General de Gaulle, 94704 Maisons-Alfort Cedex, France, www.vet-alfort.fr

3-2. Vagina; uterus; and rectum, Malignant schwannoma, rat. There is a polycystic, soft, dark brown mass with multiple foci of necrosis. Photograph courtesy of Ecole Nationale Veterinaire D'Alfort, Unite d'histologie et d'Anatomie Pathologique, 7, Avenue du General de Gaulle, 94704 Maisons-Alfort Cedex, France, www.vet-alfort.fr
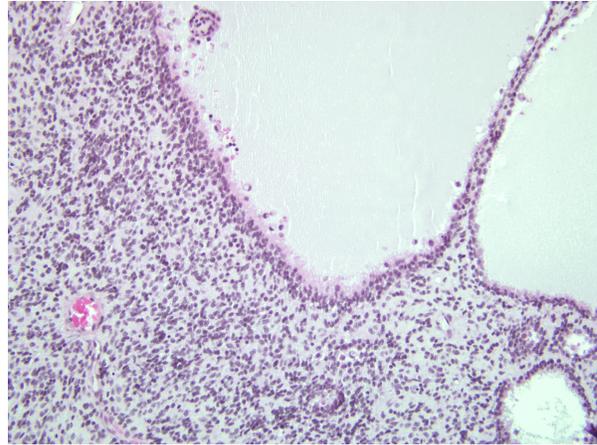
Rectum and urethra: The same neoplasm invades the serosa and the tunica muscularis of the rectum.

Immunochemistry: Specific antibodies applied to sections of the tumor revealed positive staining for vimentin, GFAP and S-100 in the cytoplasm of tumor cells. The intensity was stronger for vimentin and GFAP than for S-100.

Contributor's Morphologic Diagnosis: Vagina, uterus and rectum: Malignant schwannoma, Wistar rat, *Rattus norevegicus.*

Contributor's Comment: Classification of peripheral nerve sheath tumors is complex and various entities are recognized in human pathology: schwannoma, neurofibroma, plexiform neurofibroma, neurofibrosarcoma, malignant peripheral nerve sheath tumors, etc.[1] Because the cell of origin is often difficult to determine, and because consistent criteria are lacking, veterinary pathologists usually only classify them as benign peripheral nerve sheath tumors or malignant peripheral nerve sheath tumors.[6] However, in toxicologic pathology, the terms "benign and malignant schwannomas" are still classically used, especially in the rat.

The tumor in this case fulfills the typical morphological and immunohistochemical diagnostic criteria for uterine malignant schwannoma of the rat. The histologic appearance and demonstration of S-100 protein and GFAP by immunohistochemical procedures allow us to distinguish malignant schwannoma from the other mesenchymal neoplasms of the lower reproductive tract. Another criterion of distinction is the demonstration of basement membrane by electron microscopy.[1,7] In human pathology, two patterns are often apparent in peripheral nerve sheath tumors: Antoni A and Antoni B patterns. Antoni A pattern is composed of compact spindle cells that usually have twisted nuclei, indistinct cytoplasmic borders, and occasionally clear intranuclear vacuole. They are arranged in short bundles or interlacing fascicles. In highly differentiated Antoni A pattern areas there may be nuclear palisading, whorling of the cells and Verocay bodies (two compact rows of well-aligned nuclei separated by fibrillar cell processes). Antoni B areas are less orderly and less cellular: they are composed of spindled or oval cells arranged haphazardly within the loosely textured matrix, which is punctuated by microcystic change, inflammatory cells, and delicate collagen fibers. As in Antoni B pattern areas the schwann cells possess increased number of lysosomes and myelin figures and the basal lamina is fragmented; the Antoni B pattern could be a degenerated Antoni A pattern.[5] Rat malignant schwannomas can have areas resembling these Antoni A and Antoni B patterns.[7] The tumor in this case is characterized by numerous pseudocysts and loosely packed cells reminiscent of Antoni B pattern. The differential diagnosis of malignant schwannoma of lower reproductive tract is detailed on charts 1 and 2.[9] Spontaneous peripheral nerve sheath tumors are rare in rats.[1] Malignant schwannomas can arise in the subcutis, stomach, heart, vagina and uterus.[1,7] In the

3-3. Vagina; uterus; and rectum, Malignant schwannoma, rat. Neoplastic cells have indistinct borders, small to moderate amounts of pale eosinophilic cytoplasm, oval to fusiform nuclei with dense chromatin and one small nucleolus. Neoplastic cells line variably-sized pseudocystic cavities that contain eosinophilic material admixed with few foamy macrophages and erythrocytes. (HE 200X)

endocardium, the differential diagnosis includes benign endocardial schwannomas, which occur more frequently. They are characterized by parallel arrays of cells, sometimes Antoni A-like pattern, and absence of prominent myocardial infiltration.[9] Endocardial schwann cell hyperplasia (neurofibromatosis) also occurs in the heart. It forms a thin layer beneath the endocardium and is well-demarcated from the myocardium; it is composed of less than 20 layers of cells.[9] In both dogs and cats, malignant peripheral nerve sheath tumors are locally invasive and may have pulmonary metastases.[6] The primary sites of benign and malignant schwannomas are the brachial plexus, the lumbosacral plexus and the subcutis in the dog whereas in the cat the neoplasms arise in the nerve roots of the lower thoracic and upper lumbar cord segments.[6] In cattle, multifocal schwannomas are common in older animals and have a predilection for the autonomic nervous system, including the epicardial plexus, thoracic and cervical sympathetic ganglia, mediastinal nerve plexus, hepatic plexus, tongue, intercostal nerves, and brachial plexus.[6]

AFIP Diagnosis: Vagina; uterus; and rectum: Malignant schwannoma (malignant peripheral nerve sheath tumor).

Conference Comment: There is marked slide variation, with some slides containing vagina and uterine horn while other sections have rectum and uterus. Conference participants commented on the abundance and prominence of the cystic structures in the tumor, and some favored the histologic diagnosis of endometriosis based on the interpretation of cystic glands within an endometrial stroma. In differentiating true cysts from pseudocysts, the conference moderator emphasized that cysts are lined by epithelial cells
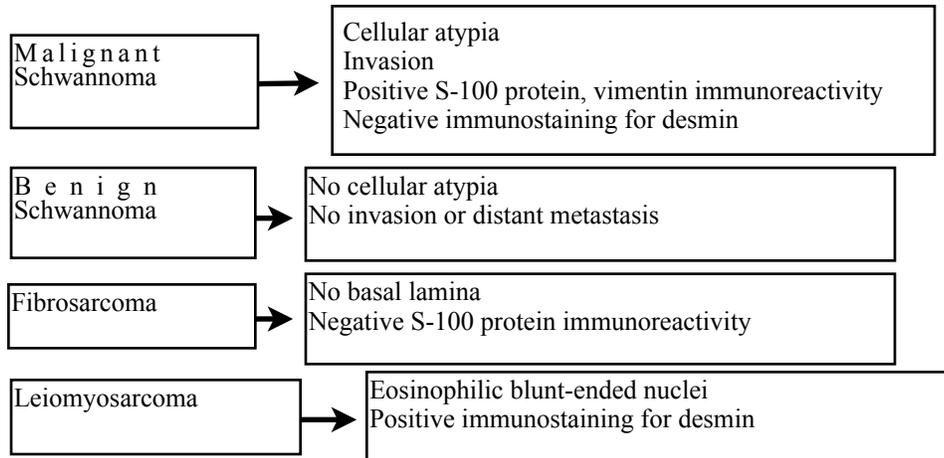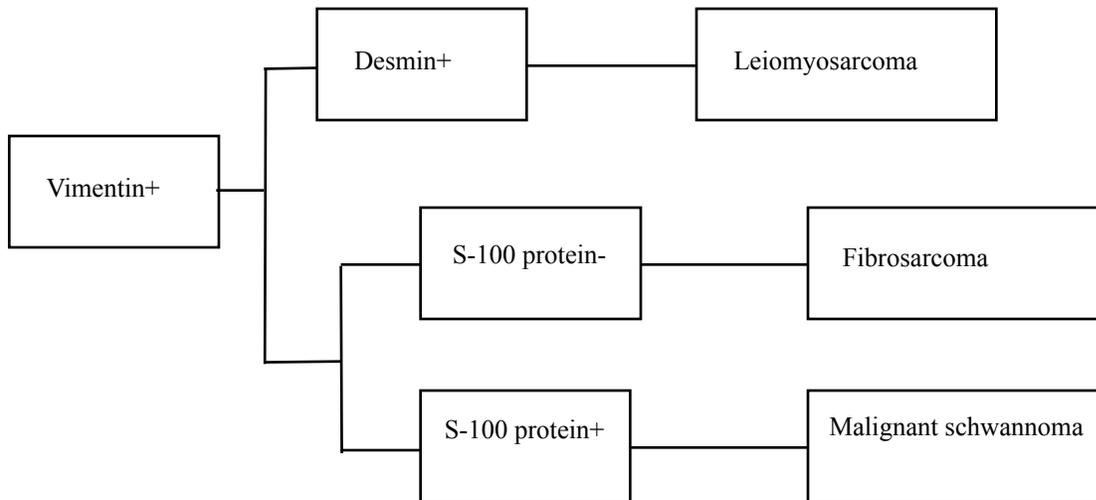
Chart 1.

Malignant Schwannoma →	Cellular atypia Invasion Positive S-100 protein, vimentin immunoreactivity Negative immunostaining for desmin
Benign Schwannoma →	No cellular atypia No invasion or distant metastasis
Fibrosarcoma →	No basal lamina Negative S-100 protein immunoreactivity
Leiomyosarcoma →	Eosinophilic blunt-ended nuclei Positive immunostaining for desmin

Chart 2.

Vimentin+
- Desmin+ → Leiomyosarcoma
- S-100 protein- → Fibrosarcoma
- S-100 protein+ → Malignant schwannoma

residing on a basement membrane. Additionally, the cells lining the cystic structures in this case are immunohistochemically positive for vimentin and negative for cytokeratin, and therefore not epithelial in origin. Additionally, while there are few reports of experimentally induced endometriosis in the rat, spontaneous endometriosis is typically a condition that occurs only in animals that menstruate, such as non-human primates.[3]

Another differential diagnosis considered by few conference participants included endometrial stromal sarcoma. This uterine tumor often invades the myometrium, cervix and nearby abdominal organs. The neoplastic cells are spindled and arranged in streams, intersecting fascicles, or whorls on a fibrillar matrix. Although areas of necrosis, inflammation and hemorrhage may be seen, cysts or pseudocysts are not typically associated with endometrial stromal sarcomas. This tumor is typically immunohistochemically positive for S-100 protein and vimentin, and negative for desmin and actin. The spindle cell neoplasm in the case of this rat is immunopositive for glial fibrillary acidic protein (GFAP), which is most consistent with a tumor of peripheral nerve origin.[2]

The contributor provides an excellent synopsis of the comparative pathology of peripheral nerve sheath tumors.

Contributor: Ecole Nationale Veterinaire D'Alfort, Unité d'Histologie et d'Anatomie Pathologique, 7 avenue du Général de Gaulle, 94704 Maisons-Alfort Cedex, France www.vet-alfort.fr

References:
1. Cardesa A, Ribalta T, Vogeley KT, Reifenberger G, Wechsler W, Turusov VS. Tumors of the peripheral nervous system. In: Turusov V, Mohr U, eds. *Pathology of Tumours in Laboratory Animals.* 2nd ed., vol 1. Lyon, France: IARC Scientific Publications; 1990:699-723.
2. Dixon D, Leininger JR, Valerio MG, Johnson AN, Stabinski LG, Frith CH. Proliferative lesions of the ovary,

uterus, vagina, cervix and oviduct in rats. *In*: Guides for toxicologic pathology; accessed at http://www.toxpath.org/nomen/index.htm, 11 August 2010. Washington D.C.: Society of Toxicologic Pathologists/American Registry of Pathology/The Armed Forces Institute of Pathology; 1999.

3. do Amaral VF, Dal Lago EA, Kondo W, Souza LC, Francisco JC. Development of an experimental model of endometriosis in rats. *Rev Col Bras Cir.* 2009; 36(3): 250-255.

4. Ellenson LH, Pirog EC: The female genital tract. In: Kumar V, Abbas AK, Fausto N, Aster JC, eds. *Robbins and Cotran Pathologic Basis of Disease.* 8th ed. Philadelphia, PA: Saunders Elsevier; 2010:1028-1029.

5. Enzinger FM, Weiss SW. *Soft tissue tumors.* St. Louis, MO: Mosby Press; 1995:829-837.

6. Koestner A, Higgins RJ. Tumors of the nervous system. In: Meuten DJ, ed. *Tumors in Domestic Animals.* 4th ed. Ames, IA: Iowa State Press; 2002:731-735.

7. Leininger JR, Jokinen MP. Oviduct, uterus and vagina. In: Boorman GA, Eustis SL, Elwell MR, Montgomery CA, MacKenzie WF, eds. *Pathology of the Fischer Rat.* San Diego, CA: San Diego Academic Press; 1990:455.

8. Mohr U. Soft tissue and musculoskeletal system. In: *International Classification of Rodent Tumours, Part I - The Rat*. Lyon, France: IARC Scientific Publications; 1992:34-36.

9. Mohr U. Central nervous system; Heart; Eye; Mesothelium. In: *International Classification of Rodent Tumours, Part I - The Rat*. Lyon, France: IARC Scientific Publications; 1992:34-37.

CASE IV: P99A (AFIP 3164426).

Signalment: 3.5-month-old, female, CB6, mouse (*Mus musculus*).

History: This mouse was a double transgene for 2 leukemogenic genes reported to be involved in acute myeloid and megakaryoblastic leukemia. During routine examination by the animal caretaker, the mouse looked sick and was sent to necropsy. It died in its cage about 2 hours after it was taken out of the animal room.
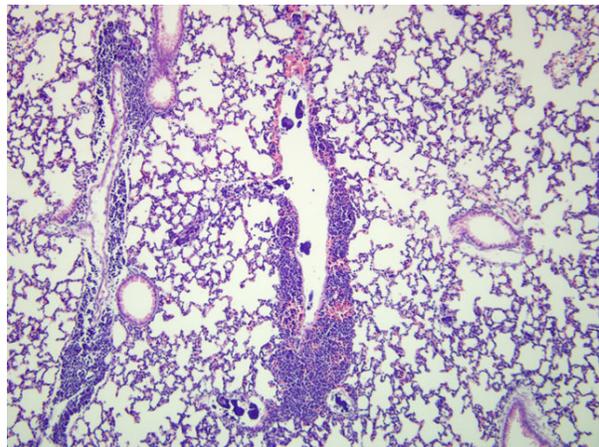
Gross Pathology: A 22.5 g female albino mouse is in rigor. The hair coat is scruffy. The tissues are pale. The gastrointestinal tract is nearly completely empty. The liver and spleen are markedly enlarged, weighing 5.2 g and 0.8 g, respectively, and 23% and 3.5% of body weight (finding age and strain-matched normal values is not easy, but in general the relative weight of the liver and spleen is approximately 4 - 5.5% and 0.2 - 0.35%, respectively). There is moderate to marked enlargement of all peripheral and visceral lymph nodes. Acute locally extensive hemorrhage is present in the mesenteric and the left axillary lymph nodes.
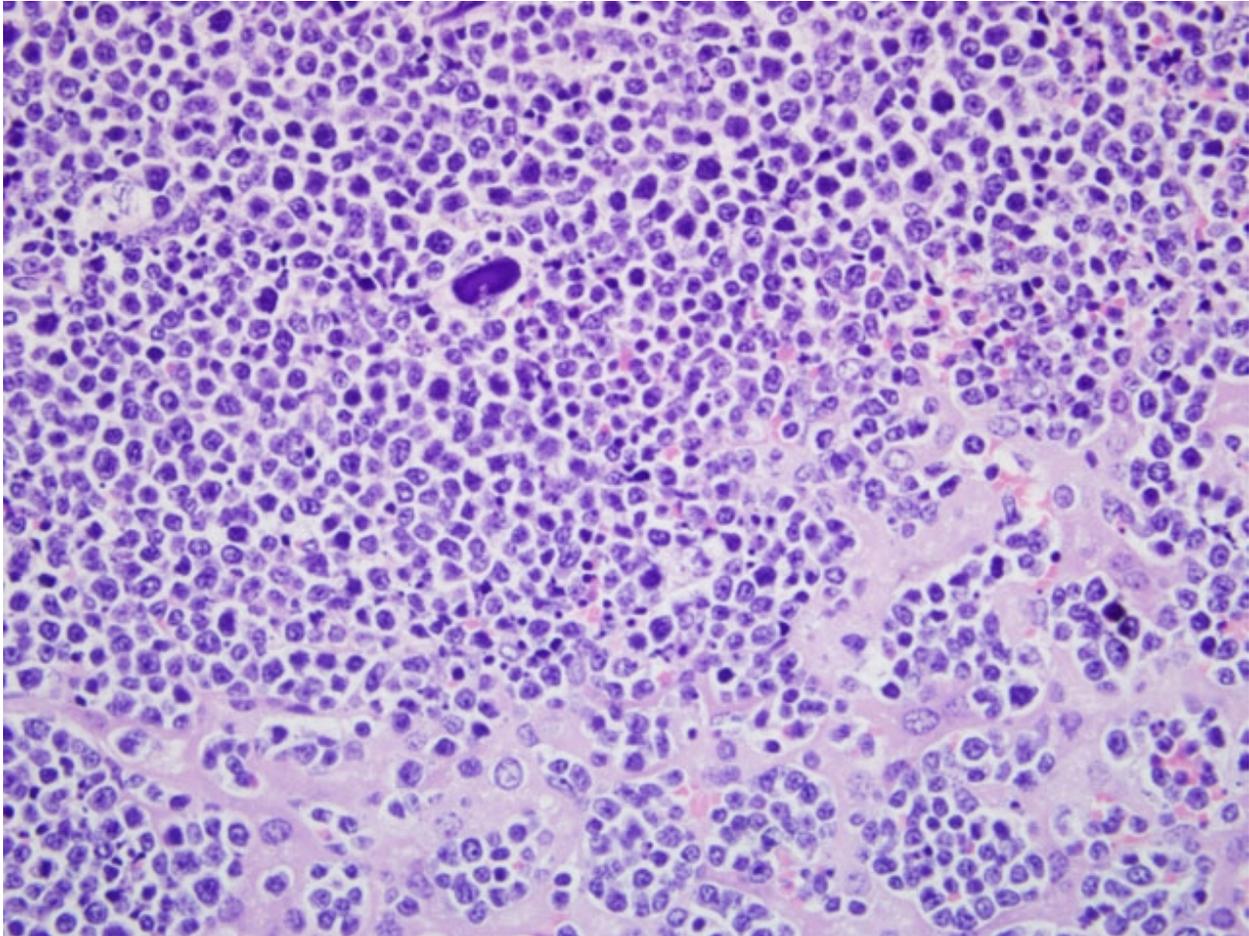
Histopathologic Description: Lung: A monomorphic population of round cells expands the peribronchiolar and perivascular interstitial tissue and is widely present in alveolar capillaries and in the lumen of blood vessels (leukemia). The neoplastic cells (blasts) are of intermediate size, approximately 1.5 – 2 fold larger than red blood cells, have a small amount of cytoplasm and round to slightly irregular coarsely granular nuclei, some with 1, or less commonly, several small nucleoli. There is mild anisocytosis and anisokaryosis. The mitotic rate is variable (0-2/HPF). Cellular debris is common. Also present in vascular lumena are numerous homogenous, acellular and deeply basophilic emboli of variable size and shape. Round to irregular emboli are especially prominent in larger blood vessels, but they are also widely distributed in alveolar capillaries. Some basophilic emboli contain a small amount of granular eosinophilic material. Non-aggregated intravascular dead cells and basophilic and eosinophilic cellular debris are also observed.

Liver: There is severe infiltration of neoplastic cells as described above. Diffusely, the cells fill and markedly expand the sinusoids and compress the hepatic plates. They form confluent aggregates, especially around large blood vessels. Cellular debris is common. Vascular lumena contain a large number of neoplastic cells and occasional basophilic emboli as described above.

Contributor's Morphologic Diagnosis: Lung and liver: Leukemia, undetermined type with widespread basophilic emboli (acute tumor lysis syndrome).

4-1. Lung, Malignant lymphoma, leukemic (Acute tumor lysis syndrome), mouse. Multifocally expanding the peribronchiolar and perivascular interstium and filling alveolar capillaries and small vessels is a monomorphic population of neoplastic lymphoid cells. Neoplastic lymphoid cells are intermediate size and have scant cytoplasm and round nuclei with coarsely stippled to clumped chromatin. Multifocally within vascular lumens are globular accumulations of homogenous, acellular deeply basophilic material (chromatin). (HE 40X)

4-2. Liver, Malignant lymphoma, leukemic (Acute tumor lysis syndrome), mouse. Neoplastic lymphoid cells fill and expand sinusoids and compress hepatocytes. (HE 400X)

Contributor's Comment: This case of a hemopoietic malignancy, still awaiting full characterization, was submitted because of the presence of multiple variably sized intravascular clumps of basophilic material. The emboli showed positive fluorescent staining with Hoechst 33342, a specific stain for AT-rich regions of double stranded DNA.[1] In this mouse, other than the liver and lung, infiltration of blasts was observed in the adrenal glands, bone marrow, connective tissue, kidney, multiple lymph nodes, ovaries, salivary glands, spleen, probable thymus and uterus. Heavy neoplastic load in conjunction with emboli of this nature is typical of acute tumor lysis syndrome (ATLS).

In humans, ATLS is caused by rapid lysis of malignant cells leading to a massive release of cellular contents. The large amount of cellular debris overwhelms homeostatic mechanisms and causes an acute metabolic crisis.[1,2,3] Spontaneous ATLS, as in this case, is rare.[1] Most cases are reported in association with aggressive chemotherapy or radiotherapy.[1,3] Acute tumor lysis syndrome is more common with hematologic malignancies than with solid tumors.[1,3] Clinically, the disorder is characterized by severe metabolic abnormalities, including hyperuricemia, hyperphosphatemia and hyperkalemia, due to substantial breakdown of nucleic acids and their release from dead tumor cells along with phosphate and potassium.[1,2,3] These abnormalities may lead to acute renal failure (the most commonly reported cause of death in human ATLS patients), bradyarrhythmias and cardiac arrest.[1,3]

In the veterinary literature, there are several case reports of chemotherapy-associated ATLS in dogs, a cat, and in a 129/SvEv mouse with PML/RARα-induced acute myeloid leukemia.[3] Spontaneous ATLS was reported in a DBA/1J mouse with leukemic lymphoma.[1] The current case is another example of spontaneous ATLS. As postulated by others, it is possible that transfer of this mouse out of the animal house led to a stress-induced surge of endogenous glucocorticoids which precipitated fatal ATLS.[1] In common with the two other murine cases, the emboli in this case were most prominent in the pulmonary vasculature.[1,3] In the case from 2003, other than the lung, emboli were identified in virtually all tissues, but were especially common in the kidney and brain.[1] In the case from 2009, emboli were observed in multiple organs, but other than the lung, were

especially prominent in the liver, as in the submitted case.[3] In the submitted case, a low number of emboli in the kidney and rare emboli in lymph nodes were also observed.

In the current case, quantification of cellular death was not undertaken. Cellular debris was common, but in our slides, the number of viable cells far exceeded that of dead cells. In the other murine report of spontaneous ATLS, necrosis affected up to 90% of tumor cells.[1] In the report from 2009, caspase-3 labeled cells are described as "plentiful."[3]

Electron microscopy was done on one of the murine cases.[1] The basophilic emboli had uniform electron dense appearance similar to that of nuclear chromatin in apoptotic lymphocytes. In mixed emboli, which at the light microscopic level had a variegated basophilic and eosinophilic appearance, the eosinophilic component was composed of aggregated cytoplasmic fragments of necrotic tumor cells.[1]

Interestingly, the authors of the 2003 report in a mouse claim to be the first to describe widely disseminated DNA and cellular debris in ATLS in humans or any other species. They ascribe this to the fact that most reports of ATLS in humans are focused on clinical management and that the few reports which describe the pathologic features of this condition are based on lesions found at death, which typically occurs several days to weeks after the onset of ATLS.[1] At that point, most reported lesions are renal and attributed to urate crystal deposition in the medulla.[1]

As noted above, in the 2003 report, emboli were identified in virtually all tissues. The authors propose that mechanical obstruction of capillary beds by these emboli plays an important role in the pathogenesis of ATLS.[1] In the more recent report of ATLS, the cause of death was postulated to be respiratory failure following massive embolization of chromatin clumps and necrotic debris in pulmonary vasculature.[3]

AFIP Diagnosis: Liver; and lung: Malignant lymphoma, leukemic, with basophilic proteinaceous emboli.

Conference Comment: Conference participants briefly discussed the pathogenesis and pathophysiologic changes of acute tumor lysis syndrome (ATLS). The syndrome is typically associated with tumors displaying rapid cell proliferation, which are typically more susceptible to chemotherapeutic agents. A recent paper cites prior studies in which 5% of humans with hematologic malignancies and 25% of high-risk patients (e.g. those with T-cell acute lymphoblastic leukemia and Burkitt's lymphoma) developed clinically apparent ATLS.[4] This finding is consistent with observations in one study in which all ATLS animals had lymphoblastic lymphoma (primarily T-cell with a few B-cell types).[4] The contributor for this case classified the malignant lymphoid neoplasm as T-cell lymphoblastic lymphoma with leukemia based on neoplastic cells demonstrating strong immunopositivity for CD3, and negative immunostaining for CD45.

The underlying cause of lysis of neoplastic cells is, as of yet, undetermined. One hypothesis is that the release of an endogenous substance may cause lysis of neoplastic cells; a suspected agent is corticosteroids, which are commonly administered for the treatment of lymphoma. Once lysed, neoplastic cells release nucleic acids, potassium, and phosphorus, resulting in the observed clinicopathologic abnormalities outlined by the contributor. The nucleic acids are broken down into their respective purine and pyrimidine components. Purines are further metabolized to uric acid, which is then converted to allantoin via urate oxidase and subsequently excreted in the urine. Interestingly, humans and non-human primates lack urate oxidase and may develop hyperuricemia and uric acid crystals within renal tubules.[4,5]

The hallmark histologic finding of ATLS is that of widely disseminated microemboli of nuclear and cytoplasmic debris.[5] Microemboli are most commonly observed in the lung, kidneys, and brain. In one study, lesions of ATLS were more common in animals found dead as opposed to those that appeared sick at the time of necropsy.[4]

Contributor: Department of Veterinary Resources, Weizmann Institute of Science, Rehovot 76100, Israel
http://www.weizmann.ac.il/vet/

References:
1. Lovelace K, Van Gessel Y, Asher LV, Vogel P. Spontaneous acute tumor lysis syndrome in a DBA/1J mouse: a case report and review. *Toxicol Pathol.* 2003;31:486-90.
2. Mylonakis ME, Koutinas AF, Papaioannou N, Lekkas S. Acute tumour lysis syndrome in a dog with B-Cell multicentric lymphoma. *Aust Vet J.* 2007;85:206-208.
3. Radaelli E, Marchesi F, Patton V, Scanziani E. Diagnostic exercise: sudden death in a mouse with experimentally induced acute myeloid leukemia. *Vet Pathol.* 2009;46:1301-1305.
4. Treuting PM, Albertson TM, Preston BD. Case series: acute tumor lysis syndrome in mutator mice with disseminated lymphoblastic lymphoma. *Toxicol Pathol.* 2010;38:476-485.
5. Vogel P, Pletcher JM, Liang Y. Spontaneous acute tumor lysis syndrome as a cause of early deaths in short-term carcinogenicity studies using $p53^{+/-}$ mice. *Vet Pathol.* 2010;47:719-724.